NORSAR

NORSAR Scientific Report No. 2-2009

Semiannual Technical Summary

1 January - 30 June 2009

Frode Ringdal (ed.)

Kjeller, August 2009

6.3 Detection Capability of IMS Primary and Auxiliary Seismic Stations

(sponsored by US Army Space and Missile Defence Command, Contract No. W9113M-05-C-0224)

6.3.1 Abstract

We have investigated the Reviewed Event Bulletin (REB) of the International Data Centre (IDC) for the time period 13 June 1999 to 15 July 2009 to quantify the event detection capability of individual seismic stations of the International Monitoring System (IMS). For a specific target area, we can obtain estimates of the detection threshold of a given station by considering the ensemble of REB reported events in the area, and simply downscaling each event magnitude with the observed SNR at the station. However, there are some factors that must be considered, such as:

- Correcting for possible biases in the REB magnitudes caused by non-detections (by using maximum likelihood estimates)
- Correcting for skewness in the distribution of threshold estimates, also caused by non-detections
- Considering the validity of using the signal-to-noise ratio for downscaling the event magnitude

We address these issues by dividing the events into a binned global grid system and introduce a data censoring procedure to reduce these effects. A major result of this study is a quantification and ranking of the IMS primary and auxiliary seismic stations based on their capability to detect events within regional, teleseismic and core phase distance ranges. For each station, source regions with noticeable signal amplitude focusing effects (bright spots) and defocusing effects are conveniently identified and quantified. We also present results from applying maximum likelihood magnitude estimation techniques for validation of the censoring procedure.

6.3.2 Data Processing and Location

Assessments of seismic network detection capabilities are usually based upon assuming statistical models for the noise and signal distributions. Subsequently, a combinational procedure is applied to determine the detection threshold as a function of the number of phase detections required for reliable location (Sykes and Evernden, 1982; Harjes, 1985; Hannon 1985; Ringdal, 1986; Sereno and Bratt, 1989). If available, station corrections for signal attenuation can be included in these computations.

As an example, Figure 6.3.1 shows detection capability of the IMS primary seismic network in late 2007, with 38 stations sending data to the IDC. The capability is represented by the magnitude of the smallest seismic event that would be detected with a 90% probability by three stations or more. Figure 6.3.2 shows the estimated improvement over this capability that could be achieved by bringing the remaining 11 primary seismic stations into operation. No station corrections have been employed in these calculations.

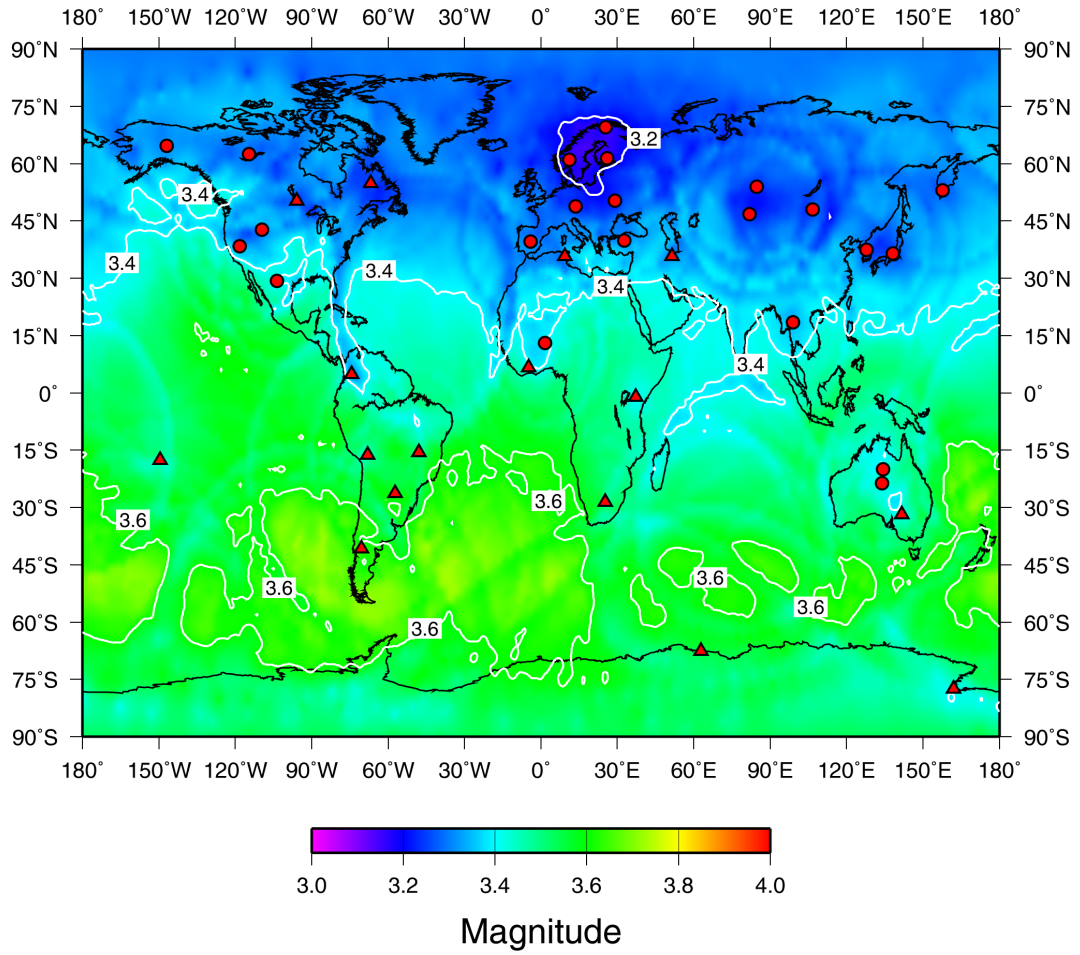

Fig. 6.3.1. Detection capability of the IMS primary seismic network in late 2007, with 38 stations sending data to the IDC. The capability is represented by the magnitude of the smallest seismic event that would be detected with a 90% probability by three stations or more. Array stations are shown as filled circles, whereas filled triangles denote three-component stations. Adopted from Dahlman et al., 2009.

While this type of maps provide a useful overview of global capabilities, they do not give a complete characterization. For example, the noise models used in these capability assessments are not able to accommodate the effect of interfering signals, such as the coda of large earthquakes, which may cause the estimated thresholds to be significantly degraded at times. Furthermore, only a statistical capability assessment is achieved, with no time-dependent evaluation of when the possibility of undetected seismic events is particularly high, for example during unusual background noise conditions or outages of key stations. Therefore, alternative methods, such as the continuous threshold monitoring technique described by Ringdal and Kværna (1989, 1992) and by Kværna and Ringdal (1999), have been showed to be useful supplements to event detection capability analysis.

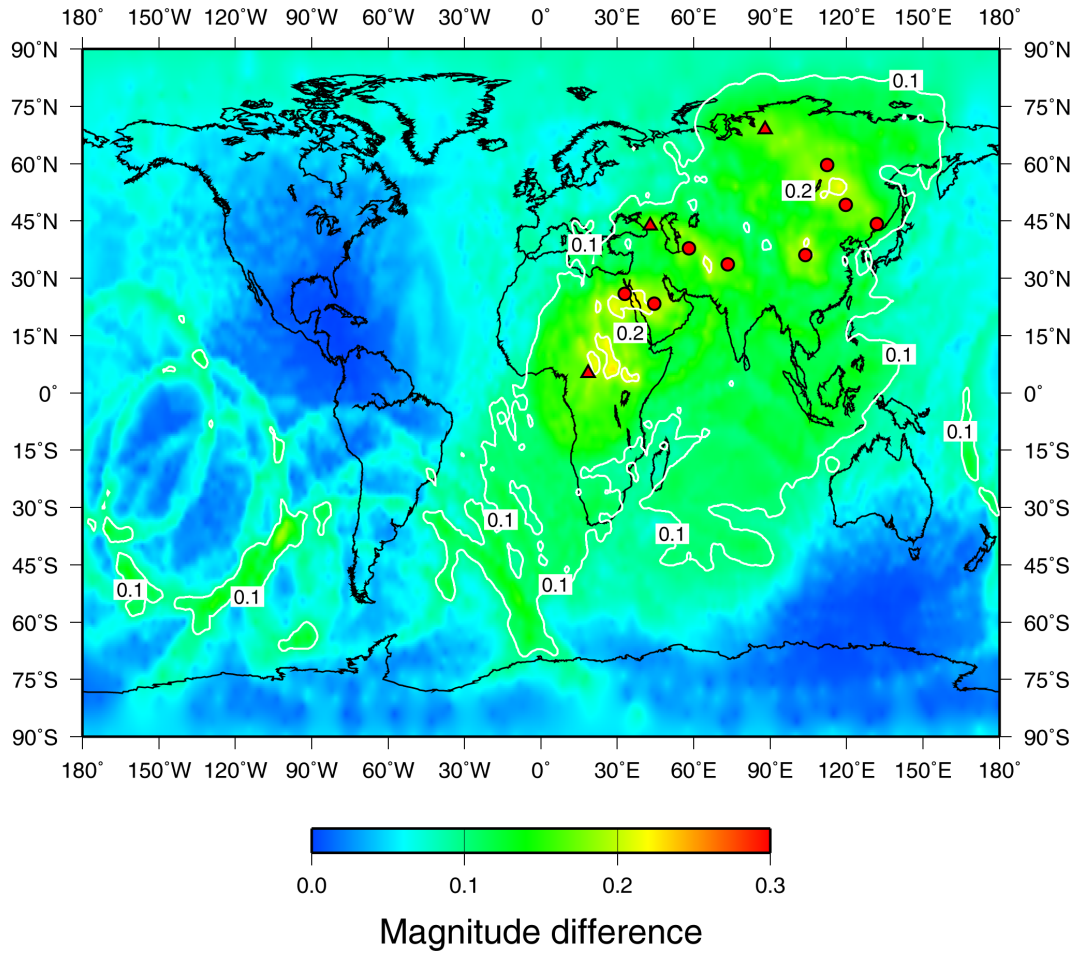

Fig. 6.3.2. Estimated improvement over the IMS capability in late 2007 that could be achieved by bringing the remaining 11 primary seismic stations into operation. Array stations are shown as filled circles, whereas filled triangles denote three-component stations. Adopted from Dahlman et al., 2009.

In this paper we address another aspect that is important for global capability estimation purposes, namely the detection capability of individual IMS stations, both on average within regional and teleseismic distance ranges, and also for specific limited source regions including regions at core phase distance ranges. As is well known, any seismic station has a detection performance that is, compared to its average performance, especially good for some regions and similarly bad for other regions. A well-known example of this is the exceptionally good performance of the NORES seismic array in Norway for detecting nuclear explosions at the former Soviet test site near Semipalatinsk, Kazakhstan (Ringdal, 1990). Additional examples are presented by Kværna et al. (2007) in their analysis of the capability to monitor North Korea's nuclear test site. The topic of the present paper is to carry out a systematic investigation of station capabilities on a regional and global basis, taking advantage of the excellent data base provided by the Reviewed Event Bulletin (REB) of the IDC for the years 1999-2009.

6.3.3 Procedure for estimating station thresholds

The database for our investigation include information about detecting and non-detecting IMS stations for events of the IDC REB. Station m_b estimates of detecting stations and noise magnitude estimates of non-detecting stations were retrieved from the IDC database in Vienna. In order to reduce the variance of the network magnitude estimates we excluded events with less than 5 stations with m_b observations in the estimates of network magnitude. In the context of CTBT monitoring, we are mainly concerned with events at shallow depths, and we therefore only considered events with reported depths less than 50 km.

We will illustrate the procedure for estimating station detection thresholds by presenting an example: As shown in Figure 6.3.3, we consider one station (ARCES) and a specific source area, in this example in China (1.5 degrees within 32°N, 104°E). Our purpose is to estimate the station detection threshold for events from this limited source area. From the REB, we obtain a large number of events, some detected by ARCES, some not detected by this station. Each event has a reference network m_b. Figure 6.3.4 shows the ARCES SNR for the detected events as a function of REB mb. We have used the REB maximum likelihood magnitudes, mbmx, in this paper. For each REB event in this source area detected by ARCES, the procedure is then to scale down the mbmx values by its log(SNR), to arrive at an instantaneous "noise magnitude" (see Figure 6.3.5). We can then add 0.5 m_b units (corresponding to SNR=3) to obtain an estimate of the instantaneous ARCES detection threshold.

Fig. 6.3.3. The source region selected for the case study presented here in centered on 32°N 104°E i China, having a radius of 1.5°, as shown by the open circle. The red curve shows the great circle path to the ARCES array in northern Norway, located at a distance of 56.4° from the center of the source region.

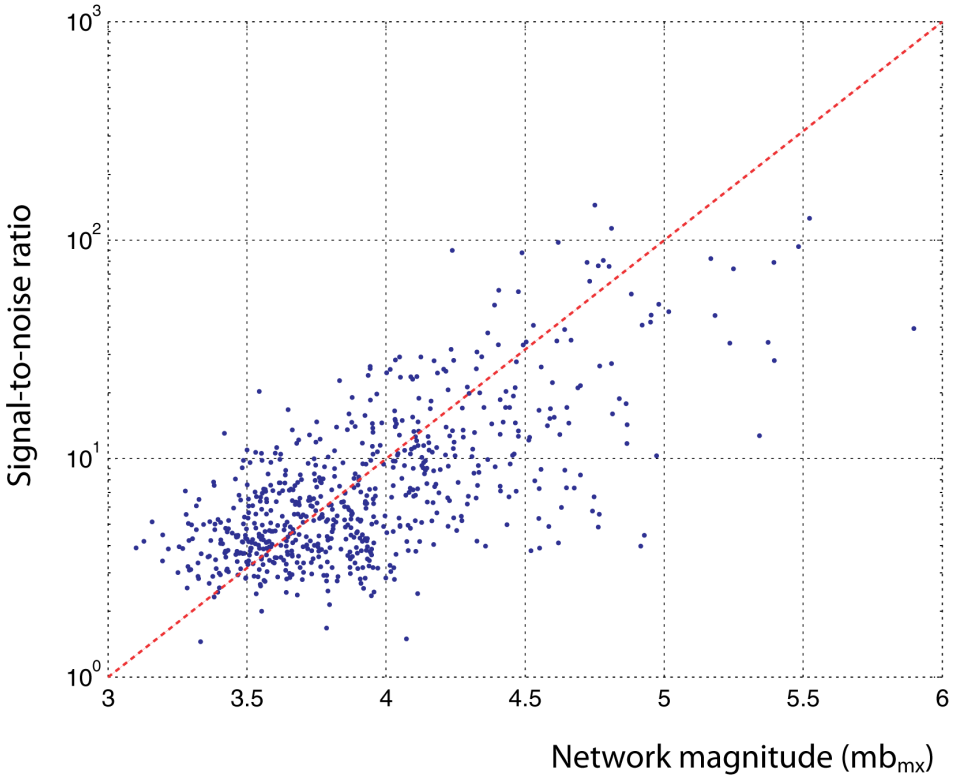

Fig. 6.3.4. Signal-to noise ratios at the ARCES array plotted as a function of REB network magnitude (mbmx) for events in the source region shown in Figure 6.3.3.

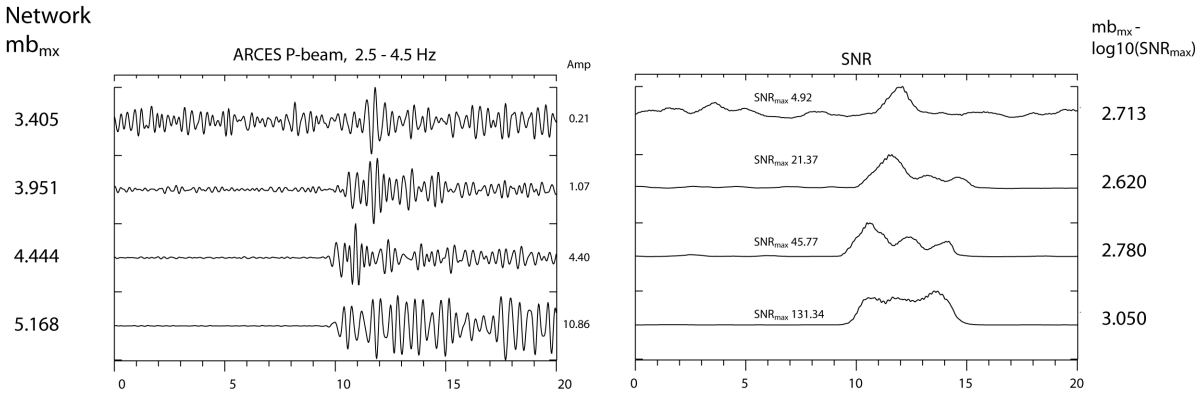

Fig. 6.3.5. Illustration of the procedure of downscaling the network magnitude mbmx by the observed log(SNR) to arrive at an instantaneous "noise magnitude" for a given region. The left-hand panel shows bandpass-filtered ARCES P-beams for 4 different events located in the source region shown in Figure 6.3.3. The corresponding network magnitudes are given to the left of the panel. The right-hand panel shows the corresponding signal-to-noise ratio (SNR) traces, together with the maximum values. The resulting estimates of the instantaneous 'noise magnitudes' of each event are given to the right of the SNR traces.

By carrying out the procedure described above for all the detected events, we obtain a set of instantaneous thresholds that clearly is magnitude dependent (see Figure 6.3.6). For each undetected event we know only that the instantaneous ARCES detection threshold must be higher than the reference network mbmx. This provides us with a classical maximum likelihood estimation framework (Ringdal, 1976). In fact, we have a number of point estimates of the instantaneous ARCES detection threshold (for those events detected by ARCES), and a number of lower bounds (corresponding to the non-detections).

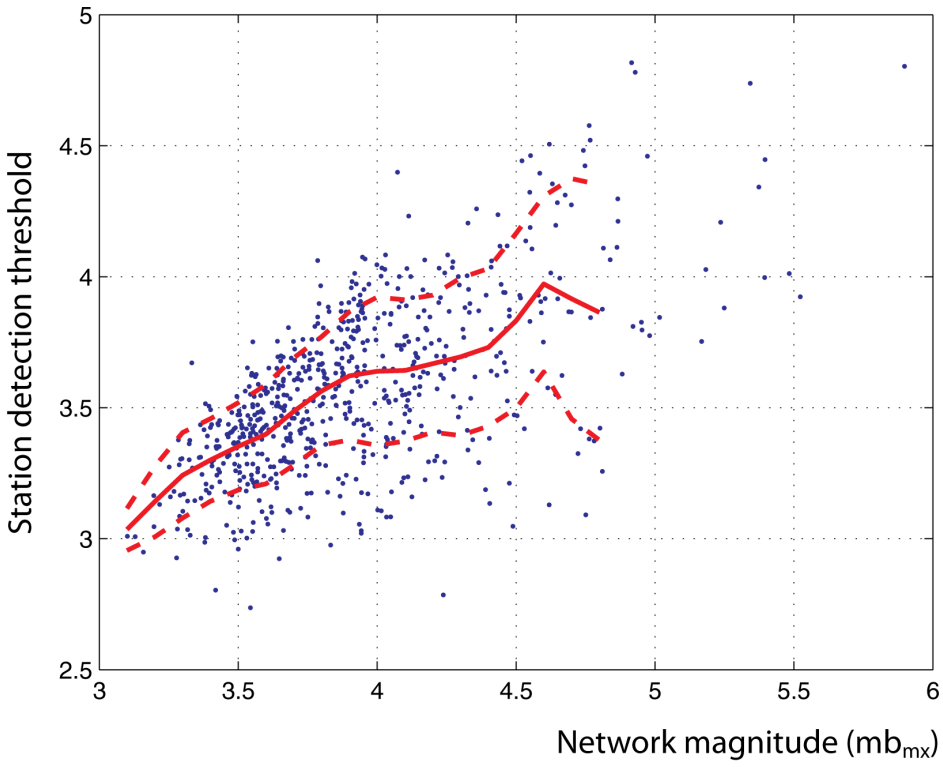

Fig. 6.3.6. The blue symbols show instantaneous detection thresholds at ARCES for events located in the source region in China (see Figure 6.3.3), using the relation of equation (1). The red line shows the running average and the dotted lines show the associated standard deviation. Notice the magnitude dependency.

The instantaneous ARCES detection threshold a_i for the *i'th* detected event is:

$$a_i = \mathrm{mbmx}_i - \log(\mathrm{SNR}_i) + 0.5 \tag{1}$$

Denoting by D the ensemble of REB events in this region detected by ARCES, we obtain the following likelihood function:

$$L(m_t) = \prod_{i \in D} \left(\frac{1}{\sigma}\right) \phi \left[\frac{(a_i - m_t)}{\sigma}\right] \prod_{i \notin D} \left\{1 - \Phi \left[\frac{\mathrm{mbmx}_i - m_t}{\sigma}\right]\right\} \tag{2}$$

Here, ϕ is the density function of the standard normal distribution and Φ is the corresponding cumulative distribution function. The symbol m_t is the ARCES detection threshold which will be estimated as the value which maximizes the likelihood function (2). We choose to keep σ constant (at a value of 0.35) although this parameter could alternatively be estimated directly from the data simultaneously with m_t.

We note in passing that the likelihood function (2) is similar to the one developed by Ringdal (1976), with the important difference that the non-detections here provide *lower bounds* rather than the *upper bounds* presented in that paper.

An illustration of the importance of taking into account non-detected events as well as the detected events is given in Figure 6.3.7. This figure shows that the fraction of non-detections increases dramatically below magnitude 4.0. As a consequence, only those events with particularly favorable path focusing effects or unusually low noise levels at the time of the event would be detected, and thus estimating the thresholds solely on the basis of these events would cause a significant bias.

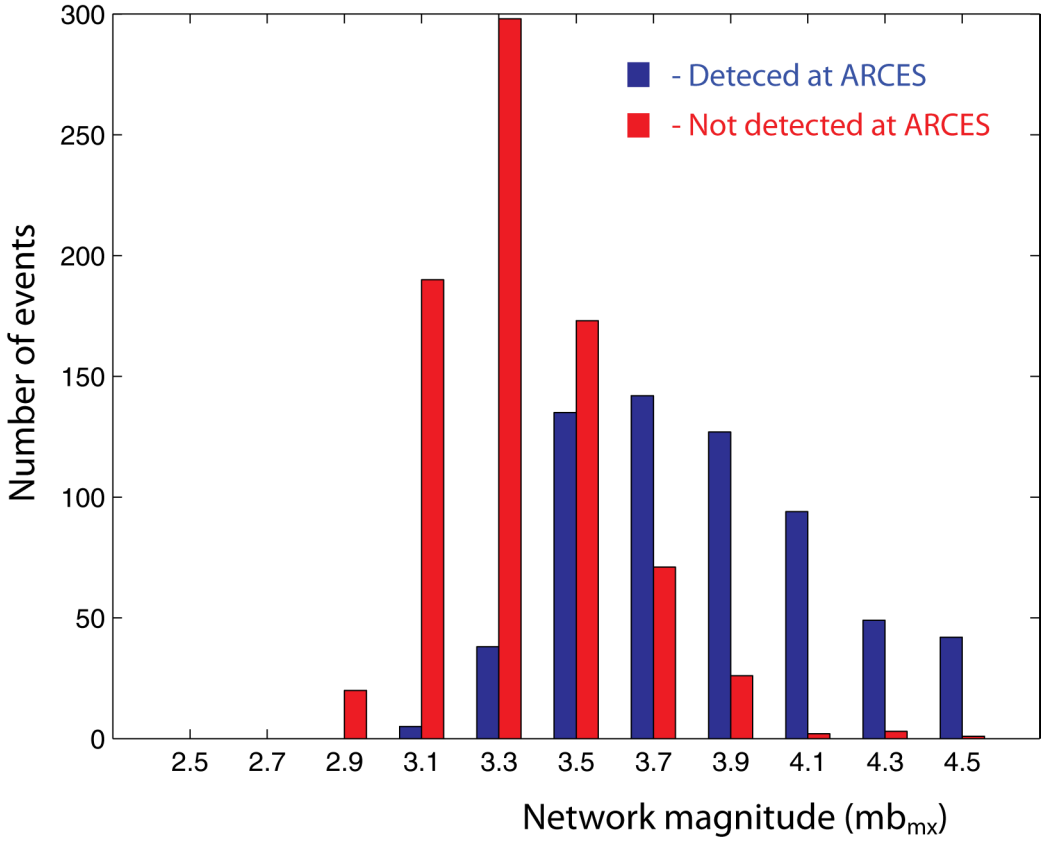

Fig. 6.3.7. Histogram of detected and non-detected P-phases at ARCES for events in the source region in China (see Figure 6.3.3).

It is now a straightforward matter to estimate the overall ARCES detection threshold for the particular site in question, using equation (2) which takes into account detections as well as non-detections. We obtain a threshold of 3.67 (Figure 6.3.8). We can verify that this computation is indeed not depending on event magnitude by computing the threshold as a function of reference magnitude (green line), where we use magnitude bins of 0.3 units. We see from Fig-

ure 6.3.8 that the threshold is essentially independent of the size of reference events in the m_b range 3.5-4.5. Below 3.5 and above 4.5 there are fewer events and the estimates are not as reliable. Censoring the data as illustrated in the figure gives an approximate threshold estimate, and we have used such censoring for most of the estimations done in this paper. As an indication of the consistency between the two approaches, Figure 6.3.9 shows the correspondence between the GERES detection thresholds for different regions as estimated by the maximum likelihood and the censoring algorithm.

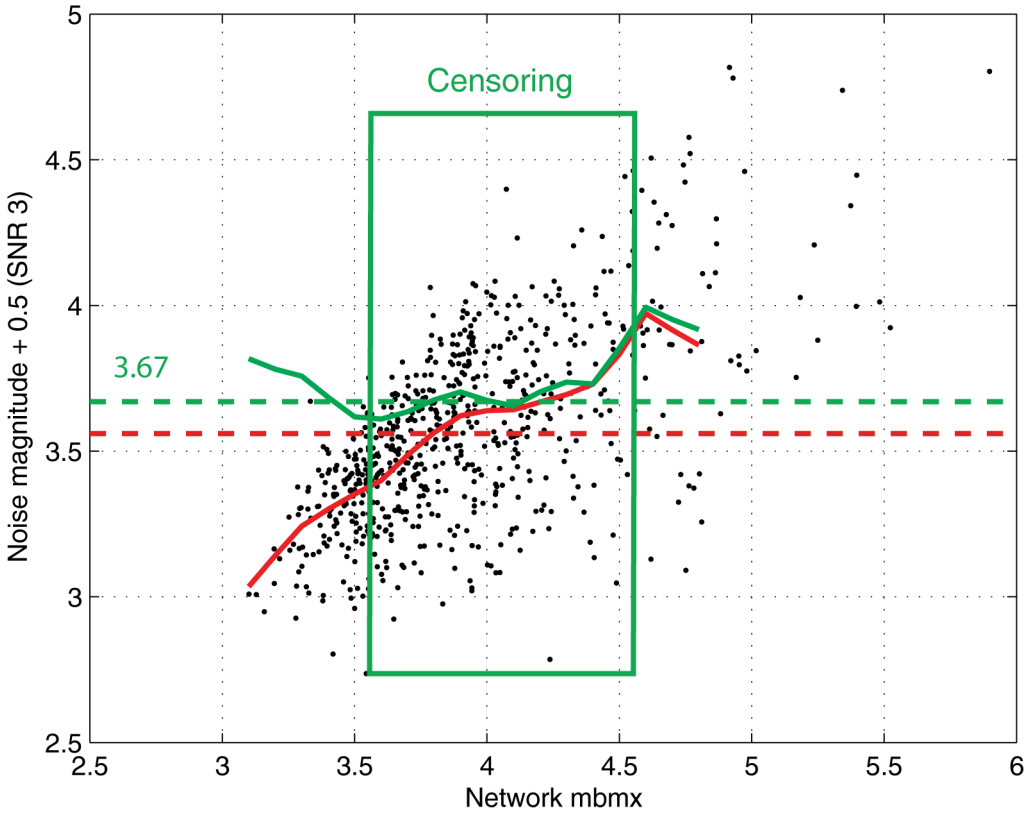

Fig. 6.3.8. The black symbols show instantaneous detection thresholds at ARCES for events located in the source region in China, and the solid red line shows the corresponding running average (similar to Figure 6.3.6). The average value for all events is 3.55 as shown by the red dashed line. The green solid line shows the maximum likelihood estimates of the detection threshold, now taking into account non-detected events, calculated in bins of 0.3 magnitude units. The green dashed line shows the maximum likelihood estimate (3.67) calculated using all events. An alternative to the maximum likelihood estimate is to censor the events used for averaging. The iterative procedure is as follows:
An initial estimate of the detection threshold is calculated from all data (the red dotted line). The average detection threshold is recalculated using only events having network magnitudes in a predefined interval around the initial estimate. In this way the smallest and the largest events, which often appear to be biased, are not included in the averaging process.

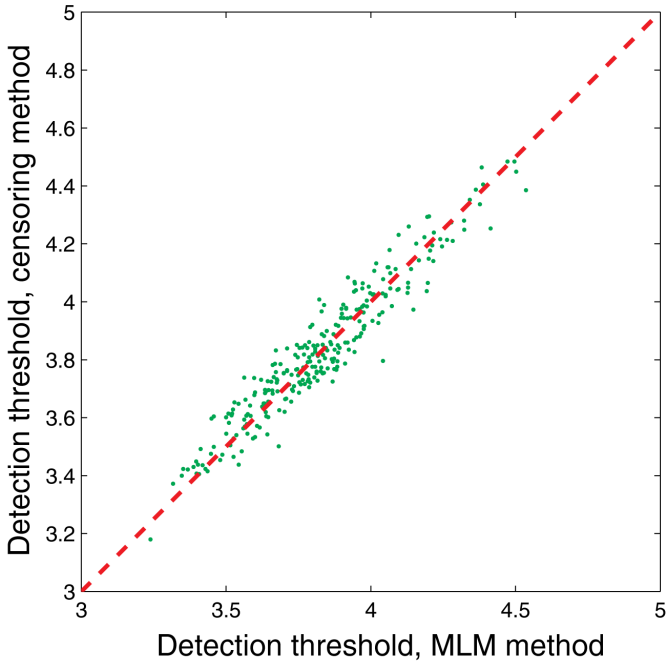

Fig. 6.3.9. The green symbols show the correspondence between the GERES detection thresholds for different regions at teleseismic distance ranges as estimated by the maximum likelihood and the censoring algorithm.

We should note here that we have not been able to apply the maximum likelihood procedure to all source-station combinations for this data set. For example, for auxiliary stations, non-detections are not reported in the REB, and thus it is not appropriate to apply the maximum likelihood procedure. Also for the primary stations, in some cases we find that the REB does not contain noise estimates for non-detections. This makes it in practice impossible for us to distinguish between cases when the lack of detection is due to station outage or to the signal being below the station threshold. In the first case, the event must be deleted in order not to skew the estimate, whereas in the second case the event must definitely be included as a genuine non-detection. In cases where maximum likelihood is not applicable, we must use the censoring approach in order to obtain threshold estimates.

6.3.4 Estimating regionalized detection threshold for a given station on a global basis

Still using the ARCES station as an example, we show in Figures 6.3.10 through 6.3.12 the ARCES regionalized detection thresholds inferred from the REB database during 1999-2009. Figure 6.3.10 indicates the number of events detected by ARCES in each 2^{o}x2^{o} bin, whereas Figures 6.3.11 and 6.3.12 show the regionalized threshold estimates in two different projections, using the censoring method. Notice that we in the following figures show the thresholds calculated without taking into account the SNR of 3.0 required for the detection. The absolute levels thus correspond to what we call the noise thresholds, i.e. SNR = 1.0. Only bins with 5 or more events remaining after applying the censoring procedure are plotted. The scale goes from better than 1.5 (violet) to worse than 4.5 (red). Not surprisingly, the capability is best at local

and regional distances (this applies of course to all stations in the network), but there are in addition significant bright spots in parts of Central Asia and the Middle East as well as indications of excellent detection of core phases southeast of Australia.

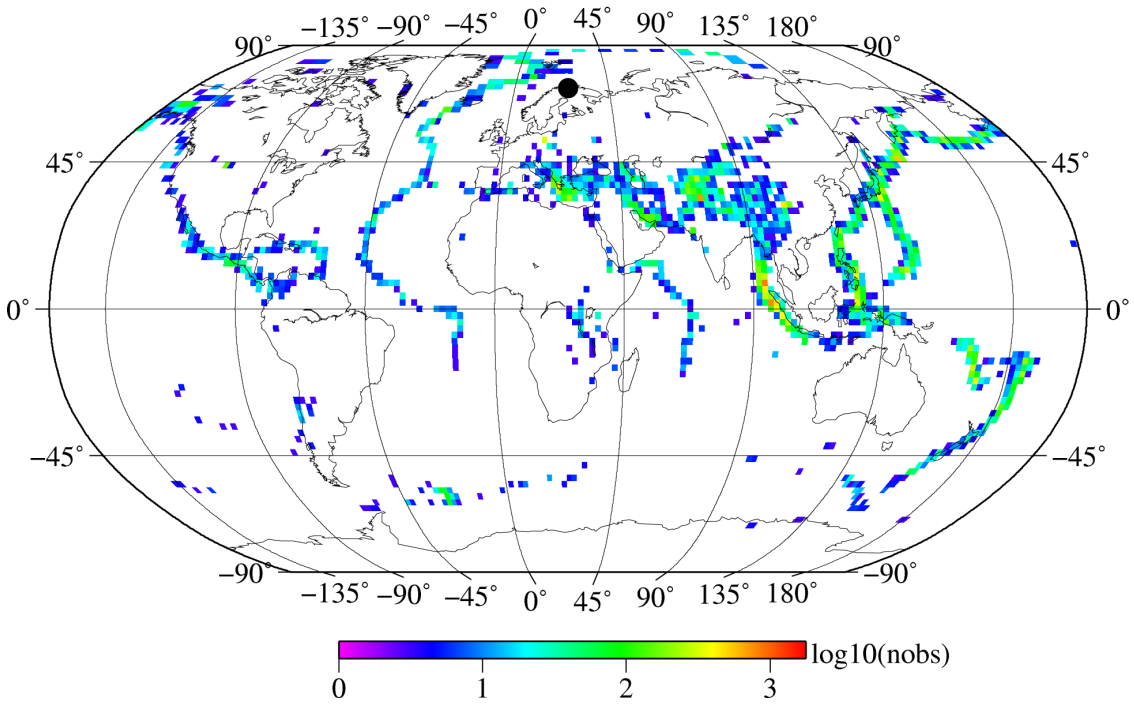

Fig. 6.3.10. The color of each $2^o x 2^o$ bin corresponds to the number of events in the REB with P-phases reported at ARCES.

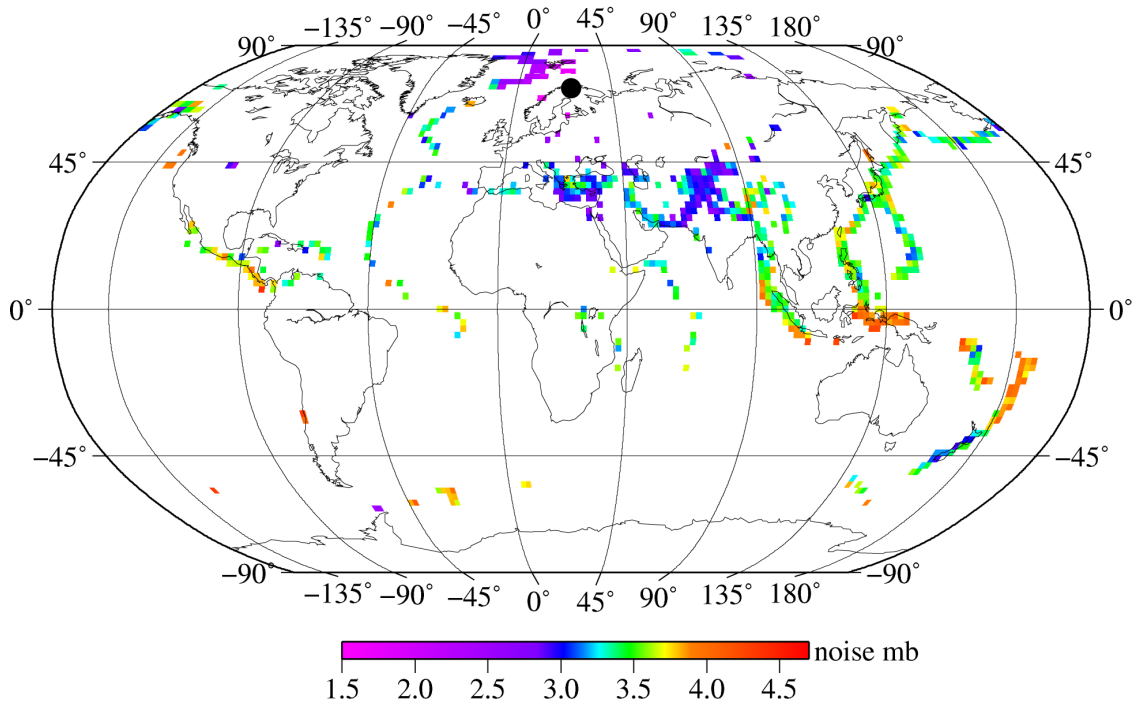

Fig. 6.3.11. Noise thresholds (SNR = 1.0) for the ARCES array in $2^o x 2^o$ bins estimated using the censoring method.

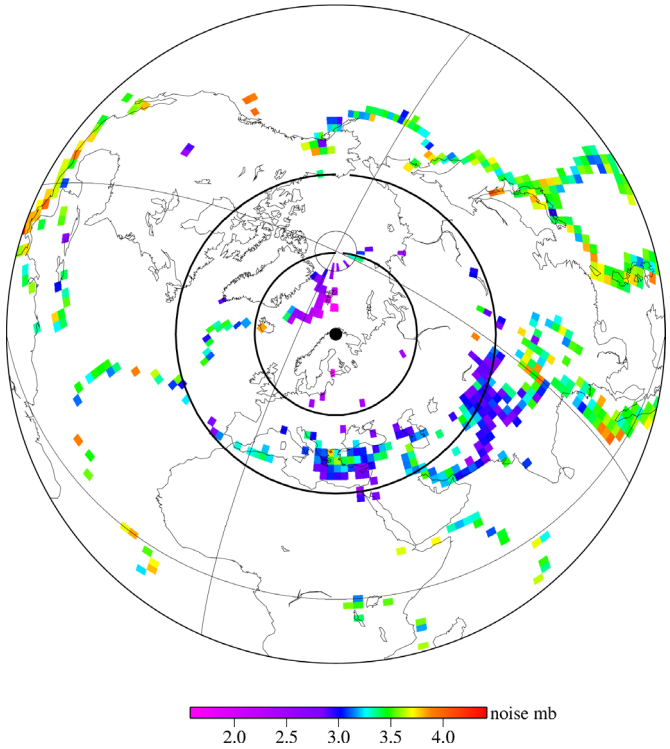

Fig. 6.3.12. Same as Figure 6.3.11, but plotted using an azimuthal projection centered around the location of the ARCES array.

6.3.5 Determining regionalized performance relative to the expected performance

As is illustrated for the ARCES array in Figure 6.3.13, a standard amplitude-distance curve can be well fitted to the estimated noise magnitudes when an average correction is applied. The standard amplitude-distance curve is similar to the curve for zero depth events used by the IDC threshold monitoring subsystem (IDC6.5.14, 2001), which combine the curves of Veith and Clawson (1972), Ringdal and Fyen (1979) and Harjes (1985) to span the full 0-180 degree distance range.

This average correction, which we in the following denote the station noise level, is in fact indicative of the overall station performance. We can use this information to determine regions where the detection performance of a given station is much better (or much worse) than its average detection performance. This is illustrated for ARCES in different map projections in Figures 6.3.14 and 6.3.15.

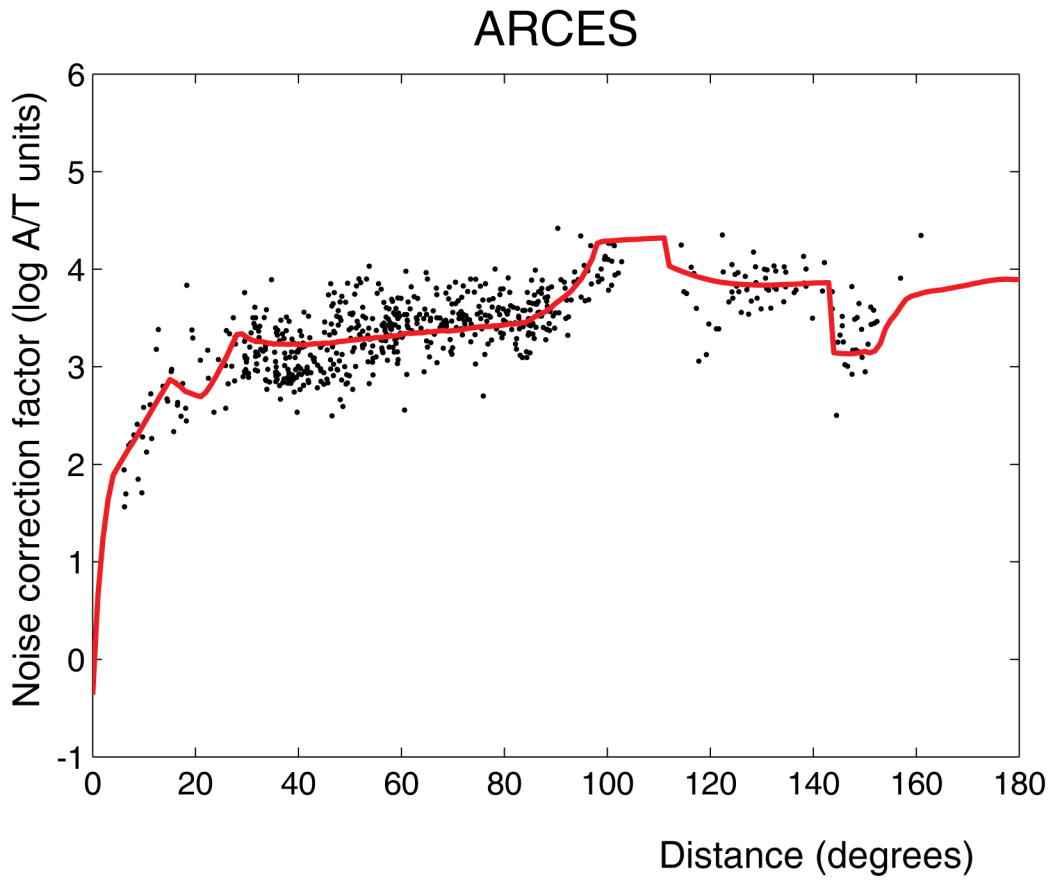

Fig. 6.3.13. The black dots correspond to the estimated noise thresholds shown in Figures 6.3.11 and 6.3.12, now plotted versus epicentral distance from ARCES. The red curve shows the best-fitting standard amplitude-distance curve.

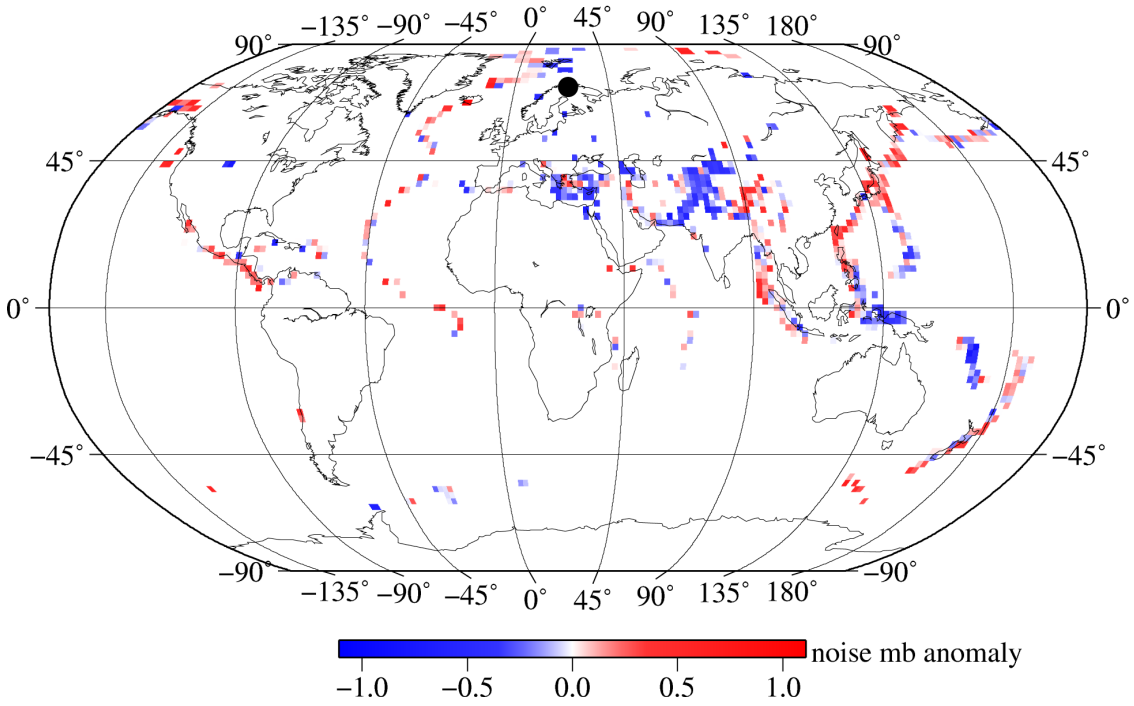

Fig. 6.3.14. Noise magnitude residuals at the ARCES array relative to the average distance dependent amplitude-distance curve shown in Figure 6.3.13. Blue indicate bins with performance better than the average ARCES performance at the corresponding epicentral distance.

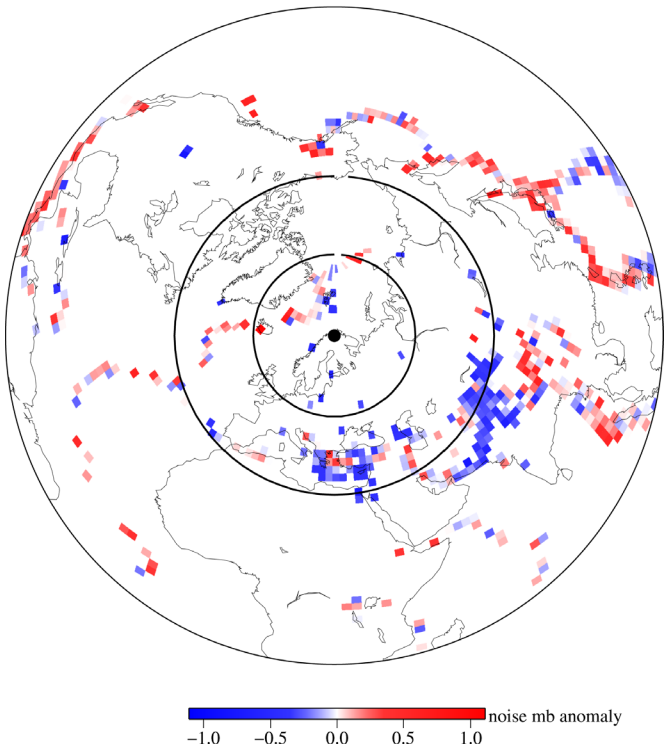

Fig. 6.3.15. Same as Figure 6.3.14, but plotted using an azimuthal projection centered around the location of the ARCES array.

As another example, an analogous picture is shown in Figure 6.3.16 for the Warramunga array in Australia. It might be important to note that in spite of the apparently less than optimum *relative* performance in the seismic belt just north of Australia (relative to the average performance expected at this close distance, given the low WRA noise level), the *absolute* performance of the array in this region is actually quite excellent (see Figure 6.3.17).

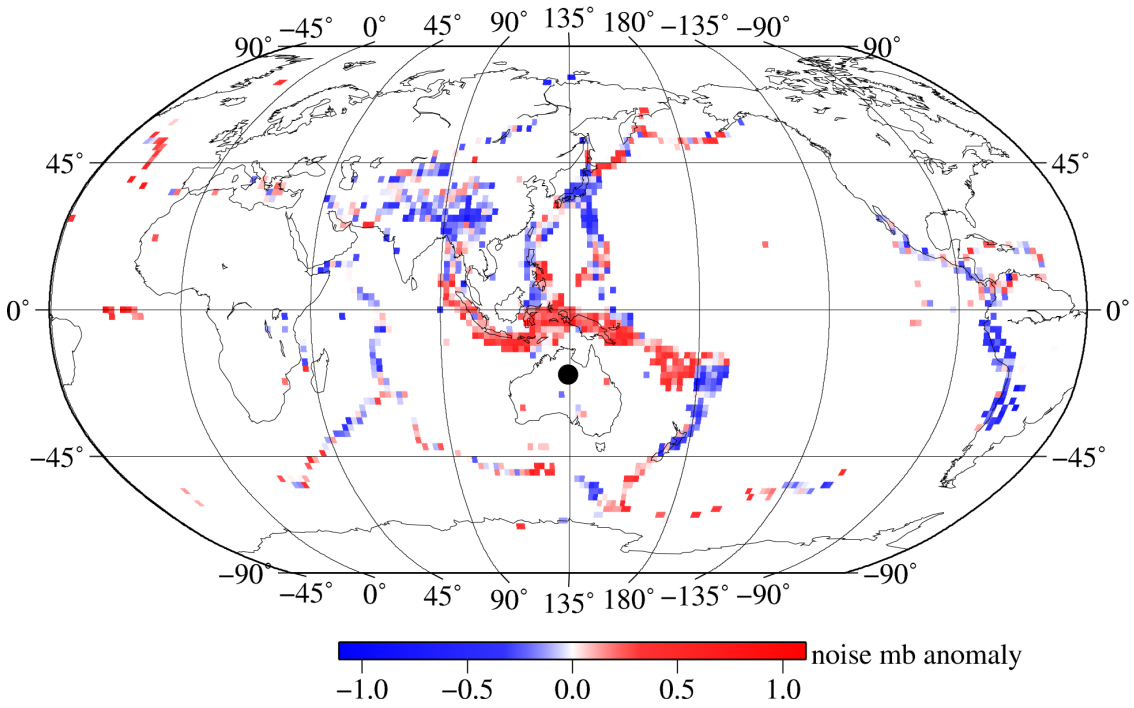

Fig. 6.3.16. Noise magnitude residuals at the WRA array relative to the average distance dependent amplitude-distance curve for the array. Blue indicate bins with performance better than the average WRA performance at the corresponding epicentral distance.

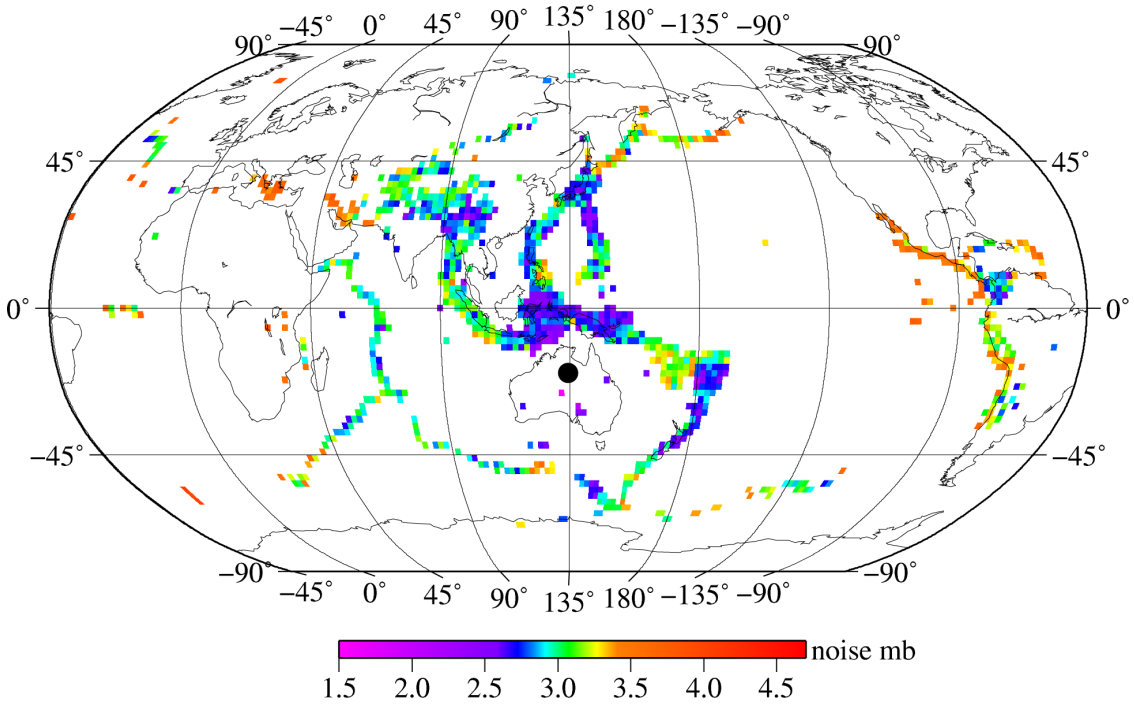

Fig. 6.3.17. Noise thresholds (SNR = 1.0) for the WRA array in $2^o x 2^o$ bins estimated using the censoring method. The blue and violet bins denote "bright spots" where the absolute performance of WRA is especially good.

It should of course be noted that the performance indicators depend on many factors, such as array design, the background noise level, the local station geology, wave propagation characteristics and also on the distance to the most active seismic zones. Furthermore, these overall capabilities are not necessarily representing the value of a given station to the IMS network. For example, some stations are situated in areas where the overall global coverage is poor, and these stations will be important contributors to monitoring events in this region, regardless of their overall performance. Additionally, as has been discussed previously in this paper, all stations have particular bright spots for detection, which may make them especially useful for selected regions.

6.3.6 Overall performance of the IMS primary and auxiliary seismic stations

As shown in Figure 6.3.13, we can for a given station fit a standard amplitude-distance curve to the noise magnitudes estimated in the different bins using an average correction factor, which we denote the station noise level. The lower the station noise level, the better is the expected station performance. Table 6.3.1 gives the estimated station noise levels for the IMS primary seismic stations for events in the teleseismic distance range 20 -95 degrees, sorted by station noise level. A bin size of $5^o x 5^o$ is used for this estimation. In order to account for the variability within each bin, the estimated station noise thresholds were projected onto the bin center using the standard amplitude-distance curve. The results obtained for the $5^o x 5^o$ and $2^o x 2^o$ bins show very good correspondence, but the benefit from using a $5^o x 5^o$ bin is that we can obtain more reliable estimates for regions with sparse seismicity. For the 20-95 degree distance range the

REB database contains information about both the SNR of the detected events as well as the instantaneous station noise magnitude of the non-detected events. This enabled us to apply the maximum likelihood estimation method, as described in section 6.3.2. For each station, Table 6.3.1 also provides the station noise levels estimated using the censoring method, also described in section 6.3.2, as well as the difference between the noise levels estimated by the two methods. Notice the good correspondence. As seen from Table 6.3.1, the arrays ASAR and WRA located in central Australia have the best overall detection performance for events in the teleseismic distance range. This excellent performance is the result of several factors like low background noise levels, efficient wave propagation and the relatively large number of array elements providing high SNR gain by beamforming. Except for the three-component station BGCA, located in the Central African Republic, the 16 best stations are, not surprisingly, all arrays. However, due to difficulties in operating the BGCA station, no data has been available after 7 January 2003. Getting the BGCA station back into operation would be of great benefit to the IMS system, and an upgrade of this station to a seismic array would possibly make it superior to all the arrays in the entire network.

For events in the regional distance range 0-20 degrees, the REB database does not contain information about non-detecting stations. It was therefore not possible to calculate maximum likelihood estimates of the noise thresholds, and we had to rely on the estimates obtained using the censoring method. The results are given in Table 6.3.2. Several of the IMS primary seismic stations are located in regions with low seismicity within regional distances. Consequently, there were for some of these stations, like BGCA and TORD - Niger, a very limited number of events available for assessment of the detection performance at regional distances. In these cases, the results should be interpreted with caution. It can also be seen when comparing Tables 6.3.1 and 6.3.2 that some of the so-called regional arrays, like ARCES and FINES in Norway and Finland, have relatively better performance for detecting events in the regional distance regime. On the other hand, it can also be seen that the performance of several of the so-called teleseismic arrays is significantly reduced. This applies in particular to large-aperture arrays like MJAR, NOA, BRTR, AKASG and CMAR, and is mainly caused by signal incoherency among the array sensors for high-frequency regional seismic signals.

The stated purpose of the IMS auxiliary seismic stations is to improve the locations of the events detected by the primary seismic network. However, several of the auxiliary stations show excellent detection performance, and we show in Table 6.3.3 the station noise levels for events in the regional distance range 0-20 degrees. It is interesting to notice that the three stations with the best performance are all located in the polar regions (SPITS - Spitsbergen, Norway, SNAA - Antarctica, RES - Resolute Bay, Canada). Stations located within the African continent (TSUM - Tsumeb, Namibia, MATP - Matapos, Zimbabwe, LSZ - Lusaka, Zambia) and in Kazakhstan (BVAR array - Borovoye, AKTO - Aktyubinsk, KURK -Kurchatov) all show excellent performance. For some of the stations, the available datasets of regional events were very small, and again, the results should be interpreted with caution. For the three stations MBAR - Uganda, MSKU - Gabon and QSPA - The South Pole, there were no 5^{o}x5^{o} bins that fulfilled the requirement of having 5 or more events for averaging after applying the censoring algorithm.

Table 6.3.1. Overall station noise levels for the IMS primary seismic stations for events in the teleseismic distance range 20-95 degrees.

Station	MLM method		Censoring method			MLM - Censoring
	Noise level	Nbin	Noise level	St. dev.	Nbin	
ASAR	-0.848	191	-0.814	0.375	180	-0.033
WRA	-0.803	207	-0.771	0.399	196	-0.032
MKAR	-0.778	210	-0.715	0.377	200	-0.063
YKA	-0.723	344	-0.689	0.433	317	-0.035
ILAR	-0.714	285	-0.714	0.344	264	0.001
TORD	-0.697	149	-0.678	0.397	126	-0.019
BGCA	-0.657	95	-0.654	0.345	75	-0.002
TXAR	-0.640	201	-0.572	0.360	183	-0.068
SONM	-0.550	325	-0.504	0.359	279	-0.046
PDAR	-0.533	245	-0.497	0.343	205	-0.036
ZALV	-0.484	237	-0.459	0.393	178	-0.025
FINES	-0.478	348	-0.438	0.385	291	-0.040
CMAR	-0.460	341	-0.484	0.361	295	0.024
NVAR	-0.440	291	-0.423	0.338	238	-0.017
AKASG	-0.433	335	-0.470	0.309	276	0.037
BRTR	-0.404	309	-0.425	0.319	237	0.021
ZAL	-0.386	360	-0.366	0.387	275	-0.020
GERES	-0.361	349	-0.389	0.328	272	0.028
ARCES	-0.348	378	-0.309	0.373	311	-0.038
LPAZ	-0.296	162	-0.296	0.337	117	0.000
NOA	-0.291	370	-0.252	0.372	275	-0.040
ESDC	-0.266	373	-0.303	0.319	303	0.037
KBZ	-0.217	90	-0.359	0.409	34	0.143
STKA	-0.162	331	-0.100	0.373	253	-0.062
KSRS	-0.148	265	-0.196	0.365	181	0.049
VNDA	-0.145	214	-0.126	0.397	157	-0.020
DBIC	-0.130	291	-0.135	0.337	184	0.005
ULM	-0.103	314	-0.066	0.333	212	-0.036
CPUP	-0.073	194	-0.069	0.333	113	-0.003
BOSA	-0.062	265	-0.080	0.344	161	0.018
SCHQ	-0.042	337	-0.006	0.348	219	-0.036
BDFB	-0.038	222	-0.035	0.315	132	-0.004
USRK	-0.032	113	-0.161	0.385	58	0.129
THR	-0.026	48	0.063	0.339	10	-0.089
PLCA	-0.011	222	0.007	0.334	109	-0.018

Table 6.3.1. Overall station noise levels for the IMS primary seismic stations for events in the teleseismic distance range 20-95 degrees.

Station	MLM method		Censoring method			MLM - Censoring
	Noise level	Nbin	Noise level	St. dev.	Nbin	
MAW	0.038	294	0.021	0.380	210	0.016
KEST	0.040	226	-0.048	0.359	102	0.088
MJAR	0.041	323	-0.006	0.344	211	0.047
PETK	0.082	181	0.089	0.401	109	-0.007
KMBO	0.179	268	0.109	0.357	128	0.070
ROSC	0.268	183	0.076	0.396	62	0.192
PPT	1.106	85	1.144	0.341	10	-0.038

Table 6.3.2. Overall station noise levels for the IMS primary seismic stations for events in the regional distance range 0-20 degrees.

Station	Censoring method		
	Noise level	St. dev.	Nbin
BGCA	-0.835	0.447	5
TORD	-0.800	0.348	1
ASAR	-0.724	0.477	11
WRA	-0.523	0.438	13
YKA	-0.506	0.501	38
FINES	-0.461	0.375	23
MKAR	-0.433	0.538	43
ARCES	-0.404	0.457	24
VNDA	-0.400	0.485	16
ILAR	-0.392	0.504	43
SCHQ	-0.364	0.496	12
TXAR	-0.295	0.493	31
ZALV	-0.277	0.529	25
PDAR	-0.263	0.505	26
GERES	-0.243	0.474	29
ESDC	-0.228	0.529	31
SONM	-0.212	0.474	38
BOSA	-0.177	0.543	14

Table 6.3.2. Overall station noise levels for the IMS primary seismic stations for events in the regional distance range 0-20 degrees.

Station	Censoring method		
	Noise level	St. dev.	Nbin
ULM	-0.170	0.395	9
ZAL	-0.170	0.499	33
NVAR	-0.043	0.451	24
CMAR	-0.016	0.507	32
KBZ	0.019	0.388	10
PETK	0.049	0.624	26
MAW	0.059	0.317	3
AKASG	0.064	0.380	28
DBIC	0.069	0.593	7
THR	0.070	0.459	9
KMBO	0.075	0.480	18
BRTR	0.076	0.447	34
LPAZ	0.094	0.519	22
STKA	0.139	0.317	5
KEST	0.152	0.550	15
KSRS	0.181	0.397	30
USRK	0.184	0.338	14
NOA	0.187	0.320	22
MJAR	0.277	0.453	31
PLCA	0.289	0.474	20
CPUP	0.354	0.450	14
ROSC	0.450	0.525	25
BDFB	0.501	0.316	2
PPT	1.353	0.404	2

Table 6.3.3. Overall station noise levels for the IMS auxiliary seismic stations for events in the regional distance range 0-20 degrees.

Station	Censoring method		
	Noise level	St.dev.	Nbin
SPITS	-0.716	0.572	32
SNAA	-0.633	0.485	17
RES	-0.568	0.545	8
TSUM	-0.545	0.476	11
BVAR	-0.480	0.373	29
AKTO	-0.368	0.354	25
MATP	-0.332	0.521	11
KURK	-0.301	0.438	29
LSZ	-0.290	0.515	18
SADO	-0.284	0.259	4
SIV	-0.280	0.503	17
FITZ	-0.258	0.616	16
LBTB	-0.238	0.526	12
INK	-0.215	0.506	32
MDT	-0.207	0.715	15
HFS	-0.182	0.491	22
SFJD	-0.152	0.393	7
EKA	-0.072	0.426	32
SDV	-0.065	0.481	27
OPO	-0.051	0.650	16
WSAR	-0.049	0.413	10
RCBR	-0.030	0.405	4
TKL	0.000	0.411	3
AAK	0.039	0.488	32
APG	0.040	0.449	5
CMIG	0.043	0.352	15
KDAK	0.071	0.518	30
SUR	0.075	0.490	14
DAVOX	0.102	0.423	20
DLBC	0.106	0.521	34
ANMO	0.116	0.482	15
ELK	0.124	0.364	20
TEIG	0.126	0.794	17
FRB	0.135	0.544	10

Table 6.3.3. Overall station noise levels for the IMS auxiliary seismic stations for events in the regional distance range 0-20 degrees.

Station	Censoring method		
	Noise level	St.dev.	Nbin
NWAO	0.137	0.503	5
BBTS	0.147	0.475	3
PCRV	0.181	0.485	14
ATTU	0.186	0.581	30
MLR	0.209	0.459	26
CFAA	0.226	0.472	19
MMAI	0.245	0.447	21
BORG	0.253	0.466	8
IDI	0.256	0.422	18
LVC	0.291	0.547	17
YBH	0.300	0.550	17
NEW	0.316	0.437	24
ATAH	0.342	0.523	18
PFO	0.351	0.478	10
DZM	0.398	0.451	24
ASF	0.422	0.406	28
JTS	0.423	0.608	18
ATD	0.425	0.506	8
EIL	0.452	0.504	29
SJG	0.453	0.465	16
JKA	0.500	0.444	33
USHA	0.512	0.539	18
RAR	0.514	0.373	8
GNI	0.524	0.448	29
RPZ	0.528	0.471	24
VRAC	0.535	0.393	23
CTA	0.544	0.379	12
PMSA	0.554	0.542	10
PALK	0.577	0.594	1
URZ	0.590	0.491	26
JNU	0.607	0.534	25
BBB	0.617	0.716	22
KAPI	0.632	0.548	20
BATI	0.640	0.530	18
LPIG	0.692	0.533	4
NNA	0.692	0.579	19

Table 6.3.3. Overall station noise levels for the IMS auxiliary seismic stations for events in the regional distance range 0-20 degrees.

Station	Censoring method		
	Noise level	St.dev.	Nbin
PMG	0.727	0.439	19
PSI	0.754	0.515	14
JMIC	0.760	0.703	12
JOW	0.768	0.499	25
VAE	0.832	0.389	11
AFI	1.011	0.437	14
HNR	1.022	0.507	13
JCJ	1.059	0.434	23
GUMO	1.105	0.476	15
JHJ	1.238	0.470	22
DAV	1.354	0.540	20
RPN	1.370	0.431	4
TGY	1.397	0.424	18
RAO	1.650	0.389	11
MBAR	-	-	-
MSKU	-	-	-
QSPA	-	-	-

Tormod Kværna
Frode Ringdal
Ulf Baadshaug

References

Dahlman, O., S. Mykkeltveit and H. Haak (2009). Nuclear Test Ban - Converting Political Visions to Reality, Springer, ISBN 978-1-4020-6883-6

Hannon, W. (1985): Seismic verification of a comprehensive test ban, Science, 227, 251-257.

Harjes. H.-P. (1985): Global seismic network assessment for teleseismic detection of underground nuclear explosions, J. Geophys., 57, 1-13.

IDC6.5.14 (2001): IDC Documentation, Threshold Monitoring Subsystem Software User Manual, SAIC-01/3004

Kværna, T. and F. Ringdal (1999): Seismic Threshold Monitoring for Continuous Assessment of Global Detection Capability, Bull. Seism. Soc. Am., 89, 946-959.

Kværna, T., F. Ringdal and U. Baadshaug (2007): North Korea's nuclear test: the capability for seismic monitoring of the North Korean test site. Seism. Res. Lett., 78/5, 487-496.

Ringdal, F. (1976): Maximum likelihood estimation of seismic magnitude, Bull. Seism. Soc. Am., 66, 789-802.

Ringdal, F. (1986): Study of magnitudes, seismicity and earthquake detectability using a global network, Bull. Seism. Soc. Am., 76, 1641-1659.

Ringdal, F. and J. Fyen (1979): Analysis of global P-wave attenuation characteristics using ISC data files. Semiann. Tech. Summ., 1 Apr - 30 Sep 1979, NORSAR Sci. Rep. 1-79/80, NORSAR, Kjeller, Norway

Ringdal, F. and T. Kværna (1989): A multichannel processing approach to real time network detection, phase association and threshold monitoring, Bull. Seism. Soc. Am., 79, 1927-1940.

Ringdal, F. (1990): Teleseismic event detection using the NORESS array, with special reference to low-yield Semipalatinsk explosions, Bull. Seism. Soc. Am., 80 Part B, 2127-2142.

Ringdal, F. and T. Kværna (1992): Continuous seismic threshold monitoring, Geophys. J. Int., 111, 505-514.

Sereno, T.J. and S.R. Bratt (1989): Seismic detection capability at NORESS and implications for the detection threshold of a hypothetical network in the Soviet Union, J. Geophys. Res., 94, 10397-10414.

Sykes, L. and J. Evernden (1982): The verification of a comprehensive nuclear test ban, Sci. Am., 247, 47-55.

Veith, K.F and G.E. Clawson (1972). Magnitude from short-period P-wave data. Bull. Seism. Soc. Am., 62, 47-55.

Appendix

A similar procedure to the one presented here for estimating station detection capability can be applied to estimating station bias β. In this case, let m_i denote the station magnitude if the *i'th* event has been detected and the station noise magnitude (upper bound) if the *i'th* event has not been detected, and define the quantity b_i by:

$$b_i = m_i - \mathrm{mbmx}_i \tag{3}$$

Denoting as before by D the ensemble of REB events in this region detected by the station, we obtain the following likelihood function:

$$L(\beta) = \prod_{i \in D} \left(\frac{1}{\sigma}\right) \phi \left[\frac{b_i - \beta}{\sigma}\right] \prod_{i \notin D} \Phi \left[\frac{b_i - \beta}{\sigma}\right] \tag{4}$$

Again, the station bias is defined as the value of β that maximizes the likelihood function. It would also here probably be appropriate to keep σ constant (at a value of e.g. 0.35) in order to increase the stability of the estimate when there are few data points, but it is clear that this parameter could be estimated directly from the data simultaneously with estimating station bias β.